

# Twist of cholesteric liquid crystal cell with substrates of different anchoring strengths

A.D. Kiselev

Chernigov State Technological University  
Shevchenko Str. 95, 14027 Chernigov, Ukraine  
Email: kisel@elit.chernigov.ua

## Abstract

We consider director configurations of cholesteric liquid crystal (CLC) cells with two plane confining substrates. Exact solutions of the Euler-Lagrange equations for out-of-plane orientations of the easy axes that correspond to inhomogeneous conical structures of CLC director are derived. We study dependence of the CLC twist wavenumber on the free twisting number assuming that anchoring energies at the substrates are either equal or different. In both cases this dependence is found to be generally discontinuous with hysteresis loops and bistability effects involved. For CLC cells with identical substrates and planar anchoring conditions the jump-like behaviour only disappears in the weak anchoring limit. Contrastingly, when the anchoring strengths are different, there is the finite value of anchoring below which the dependence becomes continuous. Another effect is the appearance of the gap between the adjacent twist wavenumber intervals representing locally stable director configurations. We calculate the critical value of anchoring asymmetry and present the results of numerical calculations.

**Key words:** cholesteric liquid crystal; anchoring energy; helix pitch; chiral strength;

**PACS:** 60.30.Dk, 60.30.Hn, 64.70.Md

## 1 Introduction

In equilibrium cholesteric phase molecules of a liquid crystal (LC) align on average along a local unit director  $\hat{\mathbf{n}}(\mathbf{r})$  that rotates in a helical fashion about a uniform twist axis [1, 2]. This tendency of cholesteric liquid crystals (CLC) to form the helical twisting pattern is caused by the presence of anisotropic molecules with no mirror plane — the so-called chiral molecules (see [3] for a recent review).

The phenomenology of CLCs can be explained in terms of the Frank free energy

$$F_b = \frac{1}{2} \int d^3x \{ K_1 (\nabla \cdot \hat{\mathbf{n}})^2 + K_2 (\hat{\mathbf{n}} \cdot \nabla \times \hat{\mathbf{n}})^2 + K_3 [\hat{\mathbf{n}} \times (\nabla \times \hat{\mathbf{n}})]^2 + 2h \hat{\mathbf{n}} \cdot \nabla \times \hat{\mathbf{n}} \}, \quad (1)$$

where  $K_1$ ,  $K_2$  and  $K_3$  are the splay, twist and bend Frank elastic constants. As an immediate consequence of the broken mirror symmetry, the expression for the bulk free energy (1) contains the chiral term proportional to the chiral strength parameter  $h$ . This parameter gives the equilibrium value of CLC twist wavenumber,  $q_0 = h/K_2$ , which corresponds to the pitch  $P_0 \equiv 2\pi/q_0$ . In what follows the parameter  $q_0$  will be referred to as the free twist wavenumber or the free twisting number. So, if the twist axis coincides with the  $z$ -direction, the director field  $\hat{\mathbf{n}} = (\cos q_0 z, \sin q_0 z, 0)$  defines the equilibrium configuration. Since  $\hat{\mathbf{n}}$  and  $-\hat{\mathbf{n}}$  are equivalent in liquid crystals, periodicity of the spiral is given by the half-pitch,  $P_0/2$ .

Typically, the pitch  $P_0$  can vary from hundreds of nanometers to many microns or more, depending on the system. The macroscopic chiral parameter  $h$  (and thus the pitch) is determined by microscopic intermolecular torques [4, 5] and depends on the molecular chirality of CLC constituent mesogenes. In experiments it can be influenced either by variations in thermodynamic parameters such as temperature or by introducing impurities.

So far we have seen that the twisting number of the ideal helical director configuration in unbounded CLCs equals the free twisting number  $q_0$ . This is no more the case in the presence of boundary surfaces or external fields that generally break the translational symmetry along the twisting axis. The case of planar CLC cell bounded by two parallel substrates exemplifies the simplest confining geometry and is of our primary concern in this paper.

Director configurations in the CLC cell are strongly affected by the anchoring conditions at the substrates, so that, in general, the helical form of the director field will be distorted. Nevertheless, when the anchoring conditions are planar and out-of-plane deviations of the director can be neglected, the configurations still have the form of the helical structure which twist wavenumber,  $q$ , differs from  $q_0$ . Dependence of the twist wavenumber  $q$  on the free twisting number  $q_0$  has been previously studied in Refs. [6, 7, 8] and was found to be discontinuous. In Refs. [9, 10] this jump-like behaviour was shown to manifest itself in abrupt changes of selective transmission spectra with temperature. Different mechanisms behind temperature variations of the pitch in CLC cells have been discussed in recent papers [11, 12].

Theoretical results of Refs. [6, 7, 8, 9, 10, 11, 12] are related to the CLC cells placed between two identical substrates and the corresponding anchoring strengths were taken to be equal. In this paper we consider CLC cells with different anchoring energies at the confining surfaces. In particular, we find that sufficiently large asymmetry in anchoring strengths will render the dependence of the twist wavenumber on  $q_0$  continuous.

The paper is organized as follows.

Director configurations within CLC cells are analyzed in Sec. 2. Using the one-constant approximation we derive exact solutions of the Euler-Lagrange equations. These solutions are expressed

in terms of the Jacobian elliptic functions and correspond to inhomogeneous conical orientational structures. The case of the planar anchoring conditions is considered in Sec. 3 where we present both analytical and numerical results about the dependence of the twist wavenumber on the free twisting number. Concluding remarks are given in Sec. 4.

## 2 Orientational structures in CLC cell

We consider director configurations in a CLC cell of thickness  $2l$  sandwiched between two parallel plane substrates located at  $z = -l$  and  $z = l$ , so that the  $z$ -axis is normal to the confining surfaces. We shall also assume that the symmetry with respect to in-plane translations is unbroken and the director field describing orientational structures does not depend on the coordinates  $x$  and  $y$ . Its parameterization in terms of the angles  $\phi$  and  $\theta$  is taken in the form:

$$\hat{\mathbf{n}}(z) = (\cos \phi(z) \cos \theta(z), \sin \phi(z) \cos \theta(z), \sin \theta(z)). \quad (2)$$

Substituting the parameterization (2) into Eq. (1) and using the one-constant approximation,  $K_i = K$ , we have the following expression for the bulk free energy per unit area:

$$F_b = \frac{K}{2} \int_{-l}^l [(\theta')^2 + (\phi' \cos^2 \theta - q_0)^2 + (\phi' \sin \theta \cos \theta)^2] dz, \quad (3)$$

where the prime stands for derivative with respect to  $z$ .

In order to specify the anchoring conditions at the boundary surfaces  $z = \pm l$  in terms of the anchoring strengths  $W_{\pm}$  and the vectors of easy orientation  $\hat{\mathbf{e}}_{\pm}$  we shall write the surface contribution to the free energy as an anchoring energy taken in the form of Rapini-Papoular potential:

$$F_s = \frac{W_+}{2} [1 - (\hat{\mathbf{n}}(l) \cdot \hat{\mathbf{e}}_+)^2] + \frac{W_-}{2} [1 - (\hat{\mathbf{n}}(-l) \cdot \hat{\mathbf{e}}_-)^2]. \quad (4)$$

The phenomenological anchoring parameters  $W_{\pm}$  characterize the strength of interaction between CLC molecules and the surfaces, while the preferred orientation of the molecules at the substrates is defined by the easy axes  $\hat{\mathbf{e}}_{\pm}$ .

### 2.1 Solutions of the Euler-Lagrange equations

The free energy functional (3) only depends on the derivative  $\phi'$ , so that the corresponding Euler-Lagrange equation can be integrated to yield the following equation:

$$\phi' = q_0(1 + c \cos^{-2} \theta), \quad (5)$$

where  $c$  is the integration constant. Variation of the functional (3) with respect to  $\theta$  will give the second Euler-Lagrange equation that can be simplified by using Eq. (5). The result is as follows

$$\theta'' = -q_0^2 \sin \theta \cos \theta (c^2 \cos^{-4} \theta - 1). \quad (6)$$

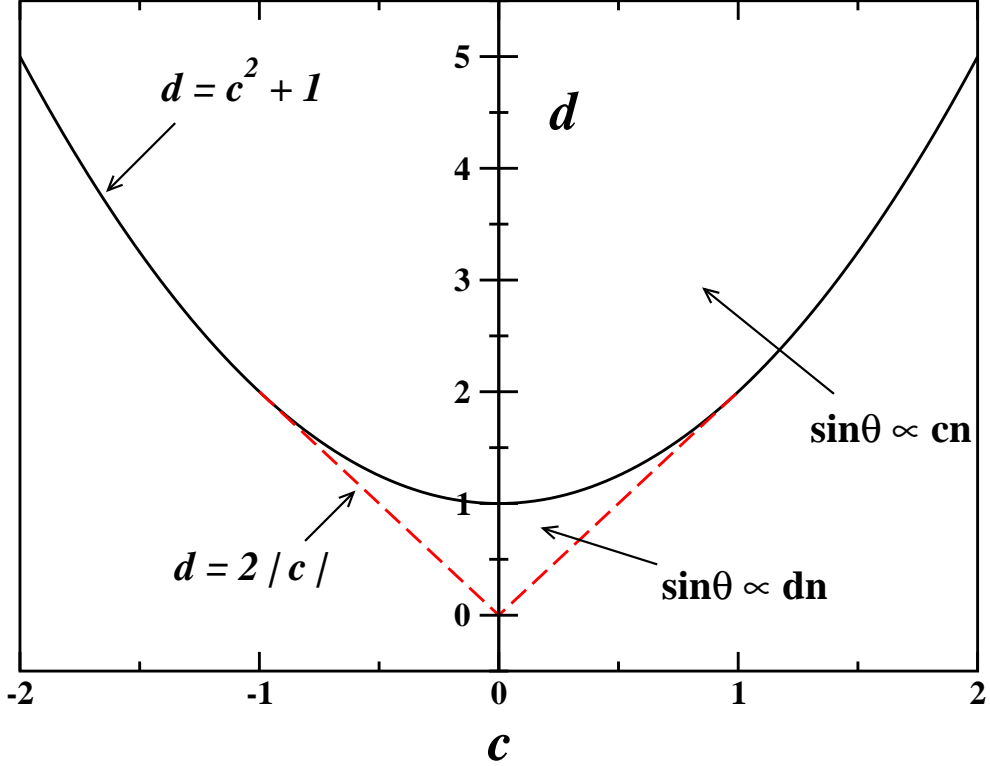


Figure 1: Real-valued solutions of Eq. (9) exist only if the integration constants  $c$  and  $d$  define a point in the  $c$ - $d$  plane that is above the curves:  $d = c^2 + 1$  at  $|c| > 1$  (solid line) and  $d = 2|c|$  at  $|c| \leq 1$  (dashed line).

The first integral of Eq. (6) is not difficult to find and is given by

$$(\theta')^2 + q_0^2(c^2 \cos^{-2} \theta + \cos^2 \theta) = q_0^2 d, \quad (7)$$

where  $d$  is the integration constant. From Eqs. (5) and (6) we have the bulk free energy in the form

$$2F_b/K = q_0^2 \int_{-l}^l (d - 2 \cos^2 \theta + 1) dz. \quad (8)$$

We can now proceed with solving Eq. (7) that can be conveniently rewritten in the form:

$$[(\sin \theta)']^2 = -q_0^2(\cos^2 \theta - c_-)(\cos^2 \theta - c_+), \quad (9)$$

where  $2c_{\pm} = d \pm \sqrt{d^2 - 4c^2}$ . This equation will have solutions only if the values of  $c_{\pm}$  are non-negative and do not exceed the unity,  $0 \leq c_{\pm} \leq 1$ . This immediately places the restriction on the parameter  $d$ :  $d \geq \max(2|c|, c^2 + 1)$ . Fig. 1 shows this region in the  $c$ - $d$  parameter plane.

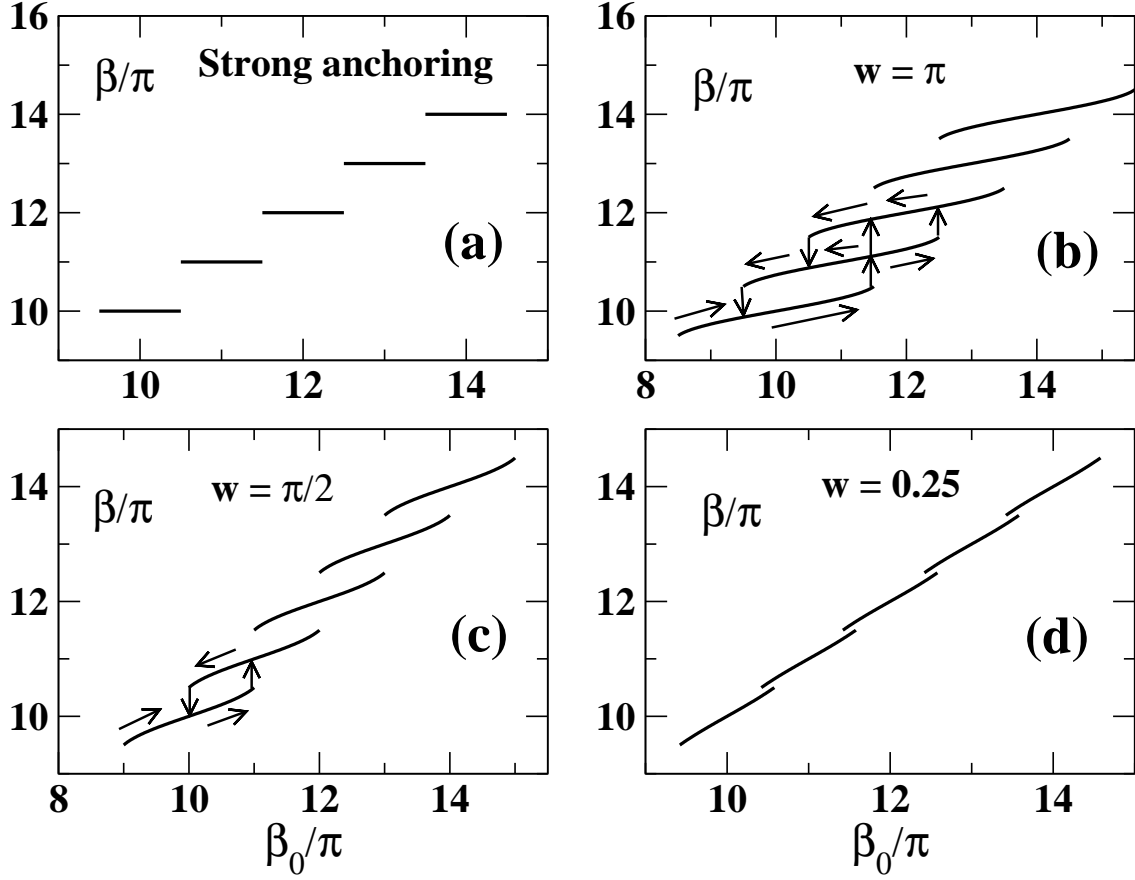


Figure 2: Dependencies of  $\beta$  ( $= 2ql - \Delta\phi$ ) on  $\beta_0$  ( $= 2q_0l - \Delta\phi$ ) at  $W_- = W_+ \equiv W$  for various values of the dimensionless anchoring energy parameter  $w$  ( $= Wl/K$ ): (a) strong anchoring limit,  $w \rightarrow \infty$ ; (b)  $w = \pi$ ; (c)  $w = \pi/2$ ; (d)  $w = 0.25$ .

In the upper part of the region,  $d > c^2 + 1$ , we have  $c_+ > 1$  and solutions of Eq. (9) can be expressed in terms of the Jacobian elliptic functions [13] as follows

$$\sin \theta = a \operatorname{cn}(bq_0z + \theta_0|m^{-1}), \quad (10)$$

where  $a^2 = 1 - c_-$ ,  $b^2 = c_+ - c_-$ ,  $m = b^2/a^2$  and  $\theta_0$  is the integration constant. Below the parabola  $d = c^2 + 1$ , where  $2|c| < d < c^2 + 1$  and  $c_+ < 1$ , these solutions are given by

$$\sin \theta = a \operatorname{dn}(aq_0z + \theta_0|m). \quad (11)$$

In addition, there are homogeneous solutions that are independent of  $z$ :  $\sin \theta = \pm\sqrt{1 - c_-}$  and  $\sin \theta = \pm\sqrt{1 - c_+}$  (at  $c_+ < 1$ ). These solutions correspond to a conical helix in which the director makes an oblique angle with respect to the helix axis. There are no spatially varying solutions at

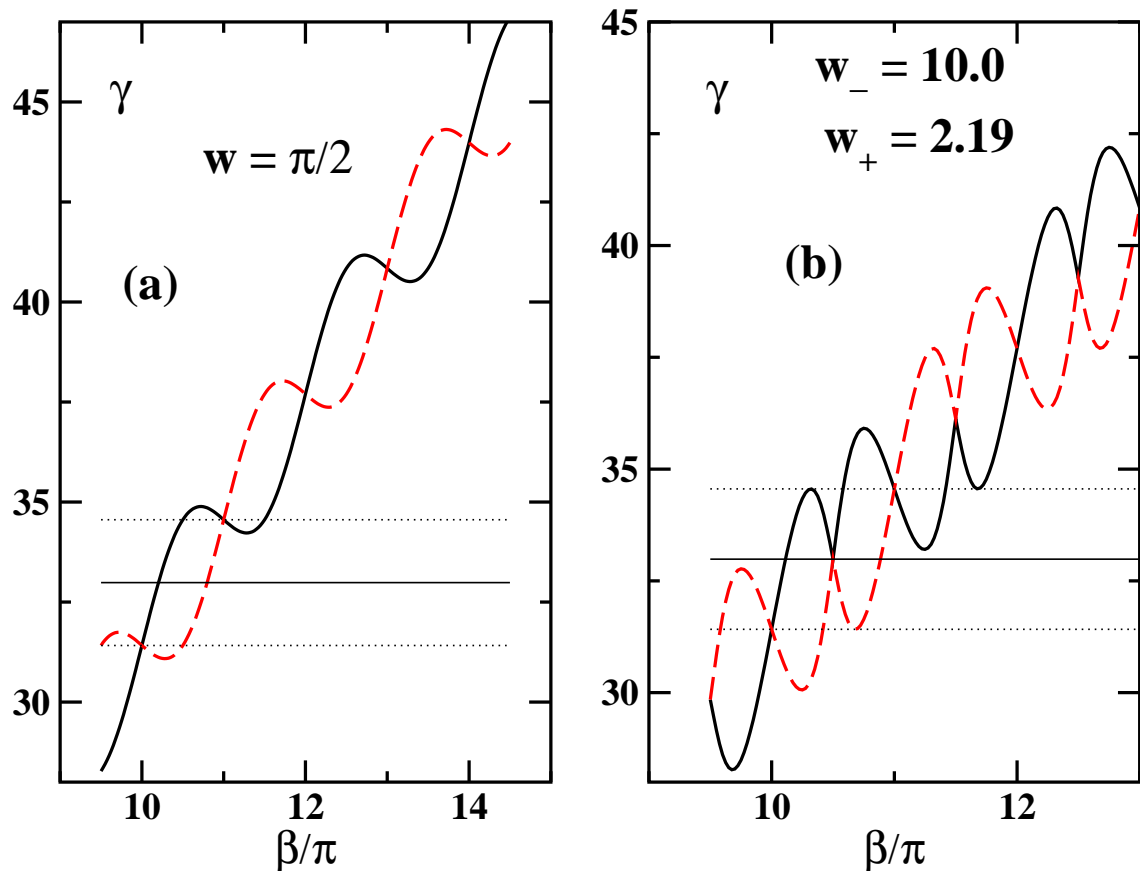


Figure 3: The curves representing the plot of the function  $\gamma_+(\beta)$  and  $\gamma_-(\beta)$  are shown as thick solid and dashed lines, respectively. The points located at the intersection of the curves and the horizontal straight line  $\gamma = \beta_0$  give the roots of Eq. (23). The value of  $\beta_0$  is  $(10 + 1/2)\pi$  (thin solid line) and is  $(10 + 1/2)\pi \pm w$  (thin dotted lines). Two cases are illustrated: (a)  $w_+ = w_- = w = \pi/2$ ; (b)  $w_- = 10.0$ ,  $w_+ = 2.19$ ,  $w = \pi/2$  (see Eq. (30)).

the boundary of the region depicted in Fig. 1. In this case the pretilt angle does not depend on  $z$  and we have

$$\sin \theta = \begin{cases} 0, & b = c^2 + 1 \text{ and } |c| \geq 1, \\ \pm\sqrt{1 - c^2}, & b = 2|c| \text{ and } |c| < 1. \end{cases} \quad (12)$$

Given the pretilt angle as a function of  $z$ , integrating of Eq. (5) will give the azimuth angle  $\phi$ :

$$\phi(z) = q_0 z + c \int_0^z \frac{q_0 dz'}{1 - \sin^2 \theta(z')} + \phi_0, \quad (13)$$

where  $\phi_0$  is the twisting angle in the middle of CLC cell.

In order to compute the integration constants  $c$ ,  $d$ ,  $\theta_0$  and  $\phi_0$  we need to know the boundary

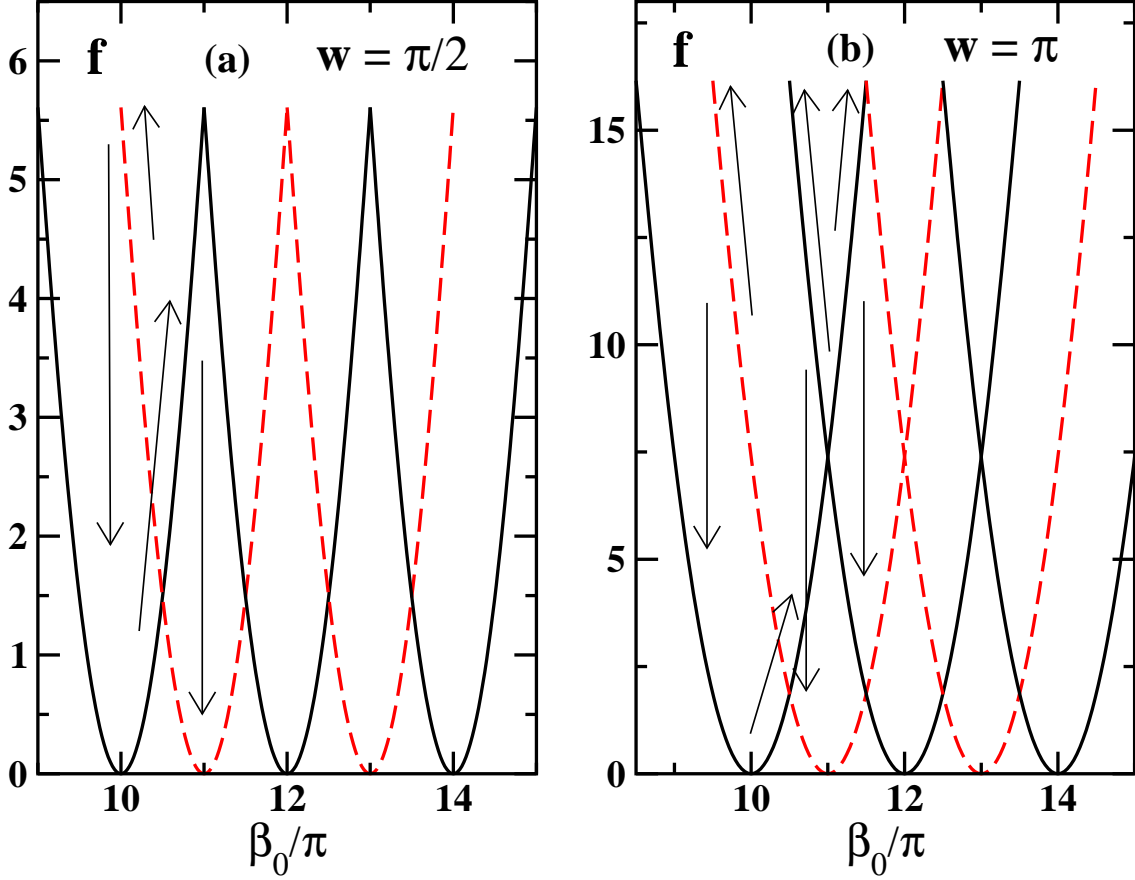


Figure 4: The free energy  $f_+$  (solid line) and  $f_-$  (dashed line) of stable configurations with the half-turn numbers between 10 and 14 as a function of  $\beta_0$  computed from Eq. (24) by using Eq. (23) for various values of the anchoring energy parameters (a)  $w = \pi/2$ ; (b)  $w = \pi$ .

conditions. The standard variational procedure will yield the following result:

$$Kq_0c = \pm W_{\pm} \cos \theta (\hat{\mathbf{n}} \cdot \hat{\mathbf{e}}_{\pm}) (\hat{\mathbf{n}}_{\phi} \cdot \hat{\mathbf{e}}_{\pm})|_{z=\pm l}, \quad (14)$$

$$K\theta'|_{z=\pm l} = \pm W_{\pm} (\hat{\mathbf{n}} \cdot \hat{\mathbf{e}}_{\pm}) (\hat{\mathbf{n}}_{\theta} \cdot \hat{\mathbf{e}}_{\pm})|_{z=\pm l}, \quad (15)$$

where  $\hat{\mathbf{n}}_{\phi} = (-\sin \phi, \cos \phi, 0)$  and  $\hat{\mathbf{n}}_{\theta} = (-\sin \theta \cos \phi, -\sin \theta \sin \phi, \cos \theta)$ .

### 3 Pitch wavenumber versus free twisting number

In this section we consider the simplest case of an ordinary spiral director configuration in which the pretilt angle equals zero,  $\sin \theta = 0$  and  $d = c^2 + 1$ . This case occurs when the anchoring conditions are planar and both of the easy axes are parallel to the confining surfaces. We direct

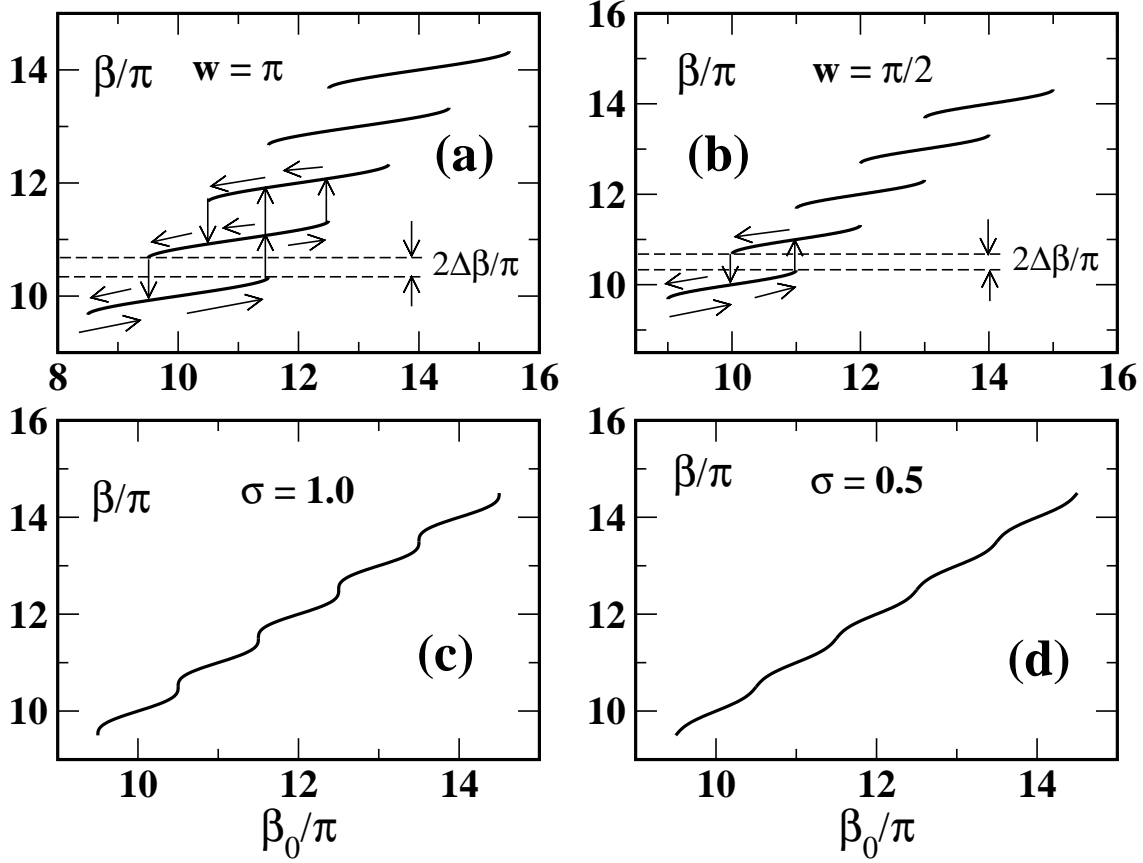


Figure 5: Dependencies of  $\beta$  on  $\beta_0$  calculated at  $w_- = 10.0$  for various values of the parameters  $\sigma$  ( $= 2w_-w_+/(w_- - w_+)$ ) and  $w$  (see Eq. (30)): (a)  $w = \pi$  ( $\sigma = 11.8$  and  $w_+ = 3.705$ ); (b)  $w = \pi/2$  ( $\sigma = 5.6$  and  $w_+ = 2.19$ ); (c)  $\sigma = 1.0$  ( $w_+ = w_c = 0.476$ ); (d)  $\sigma = 0.5$  ( $w_+ = 0.25$ ).

the  $x$ -axis along the vector  $\hat{e}_-$ , while the easy axis at the upper substrate is rotated through the angle  $\Delta\phi$ :  $\hat{e}_+ = (\cos \Delta\phi, \sin \Delta\phi, 0)$ .

From Eq. (13) we have

$$\phi = qz + \phi_0, \quad (16)$$

where  $q = q_0(1+c)$  is the twisting wavenumber. The boundary conditions (14) can be conveniently rewritten in the form:

$$\beta - \beta_0 = -w_{\pm} \sin(\beta \pm \alpha), \quad w_{\pm} \equiv W_{\pm}l/K, \quad (17)$$

$$\beta = 2ql - \Delta\phi, \quad \alpha = 2\phi_0 - \Delta\phi, \quad \beta_0 = 2q_0l - \Delta\phi. \quad (18)$$

Eqs. (17) define stationary points of the free energy written as a function of the parameters  $\alpha$  and  $\beta$ :

$$4lF(\alpha, \beta)/K = (\beta - \beta_0)^2 - w_+ \cos(\beta + \alpha) - w_- \cos(\beta - \alpha) + (w_- + w_+). \quad (19)$$



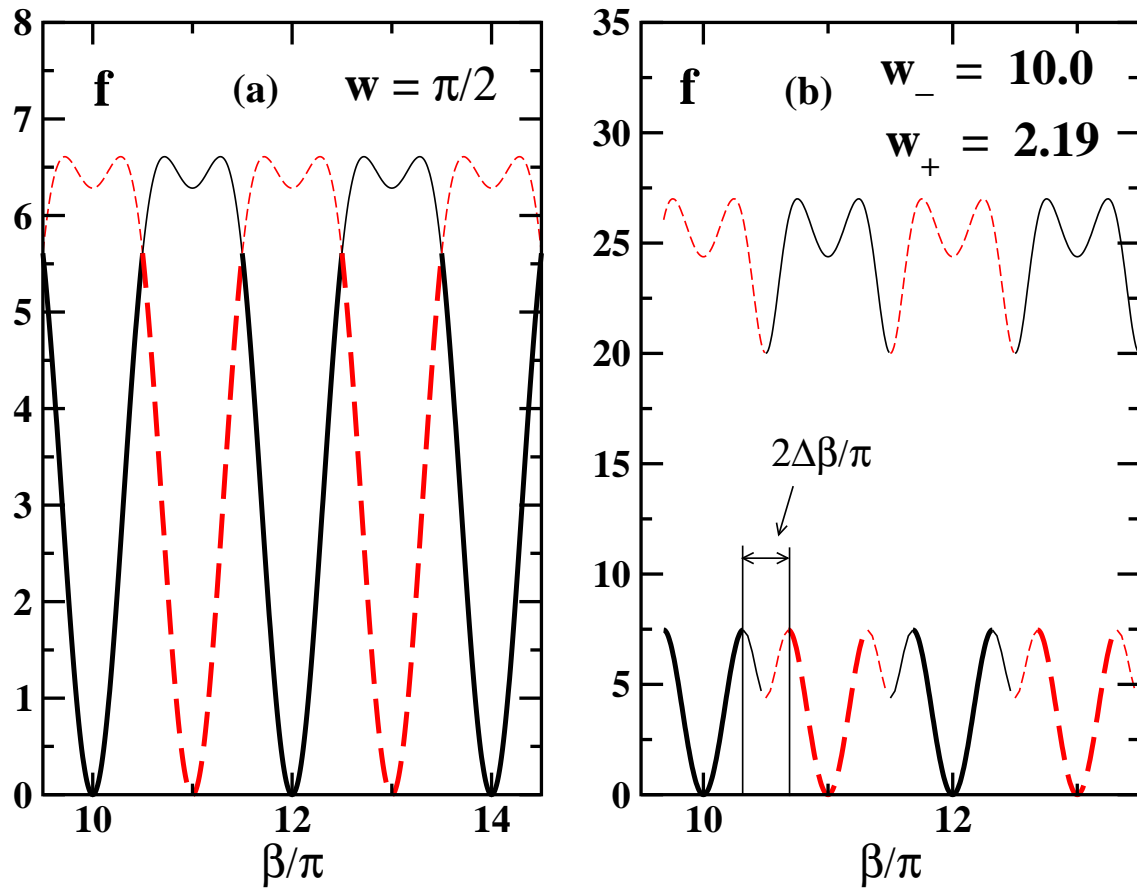


Figure 6: The free energy  $f_+$  (solid line) and  $f_-$  (dashed line) of the configurations with the half-turn numbers between 10 and 14 as a function of  $\beta$  computed from Eq. (24). Thin lines represent the energy of unstable configurations. Two cases are shown: (a)  $w_- = w_+ = w = \pi/2$ ; (b)  $w_- = 10.0$ ,  $w_+ = 2.19$  ( $\sigma = 5.6$  and  $w = \pi/2$ ).

There are two additional conditions for a stationary point to be a local minimum of the free energy surface (19). These conditions ensure local stability of the corresponding director configurations and can be written in the following form:

$$A \equiv w_+ \cos(\beta + \alpha) + w_- \cos(\beta - \alpha) > 0, \quad (20)$$

$$H \equiv A + 2w_+w_- \cos(\beta + \alpha) \cos(\beta - \alpha) > 0. \quad (21)$$

From Eq. (17) we can now relate the angles  $\alpha$  and  $\beta$  through the following equation

$$\alpha = \arctan[\epsilon \tan \beta] + \pi k, \quad \epsilon = \frac{w_- - w_+}{w_- + w_+}, \quad (22)$$

where the number  $k$  is integer,  $k \in \mathbb{Z}$ , that is the number of half-turns of the spiral. Substituting

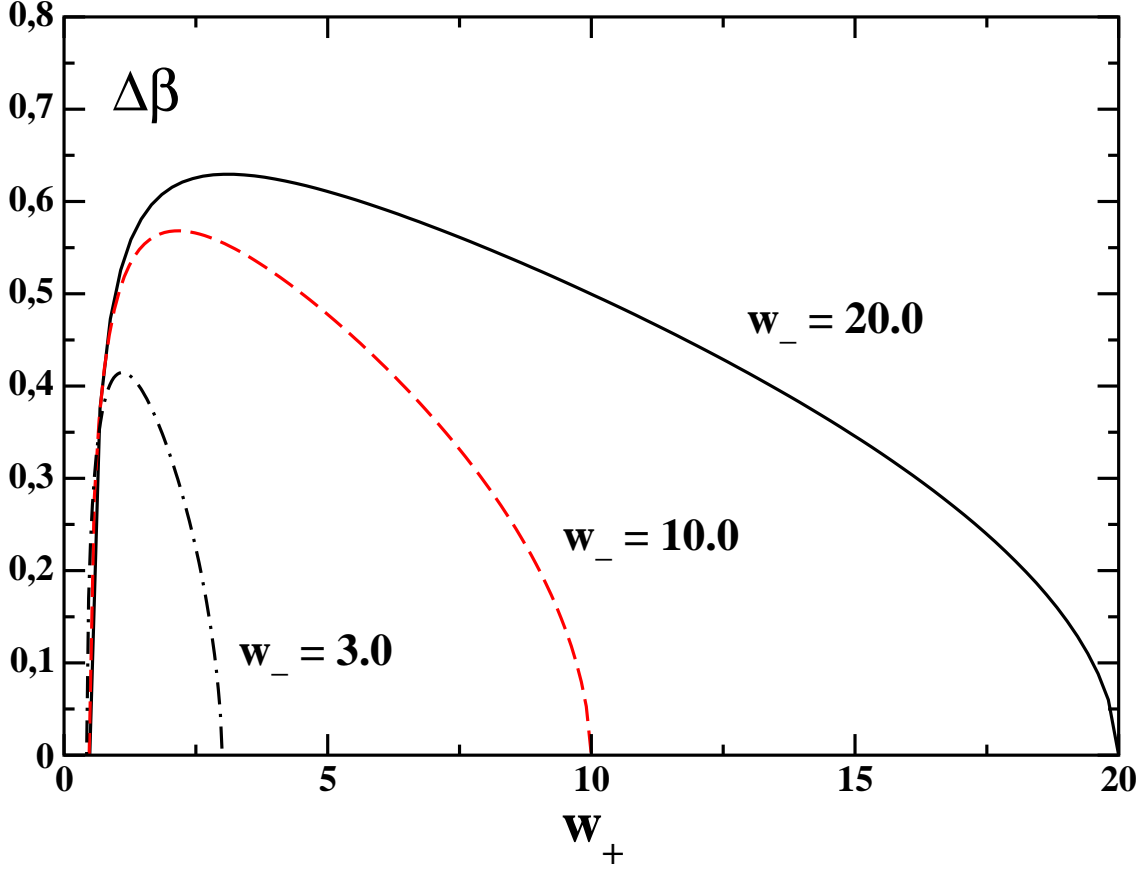


Figure 7: Dependencies of  $\Delta\beta$  on  $w_+$  for various values of the anchoring energy parameter  $w_-$ .

the relation (22) into Eq. (17) will give a pair of transcendental equations for  $\beta$ :

$$\beta_0 = \gamma_{\pm}(\beta) \equiv \beta \pm w_+ \sin(\beta + \arctan[\epsilon \tan \beta]) . \quad (23)$$

The right hand side of Eq. (23) is  $\gamma_+(\beta)$  ( $\gamma_-(\beta)$ ) when the number  $k$  is even (odd). Solving Eqs. (23) will provide, in general, various values of  $\beta$ . The values that meet the stability conditions (20) and (21) correspond to metastable configurations of CLC. The equilibrium director structure is determined by the solutions of Eq. (23) that give the least value of the free energy. From Eqs. (19) and (23) the free energy can be expressed in terms of the angle  $\beta$  and is given by

$$4lF_{\pm}(\beta)/K \equiv f_{\pm}(\beta) = w_+^2 \sin^2 \psi_+ \mp (w_+ \cos \psi_+ + w_- \cos \psi_-) + (w_- + w_+) , \quad (24)$$

$$\psi_{\pm} \equiv \beta \pm \arctan[\epsilon \tan \beta] . \quad (25)$$

Similarly, we can use Eq. (22) to rewrite the stability conditions as follows

$$A_{\pm} \equiv \pm(w_+ \cos \psi_+ + w_- \cos \psi_-) > 0 , \quad (26)$$

$$H_{\pm} \equiv A_{\pm} + 2w_+w_- \cos \psi_+ \cos \psi_- > 0 . \quad (27)$$

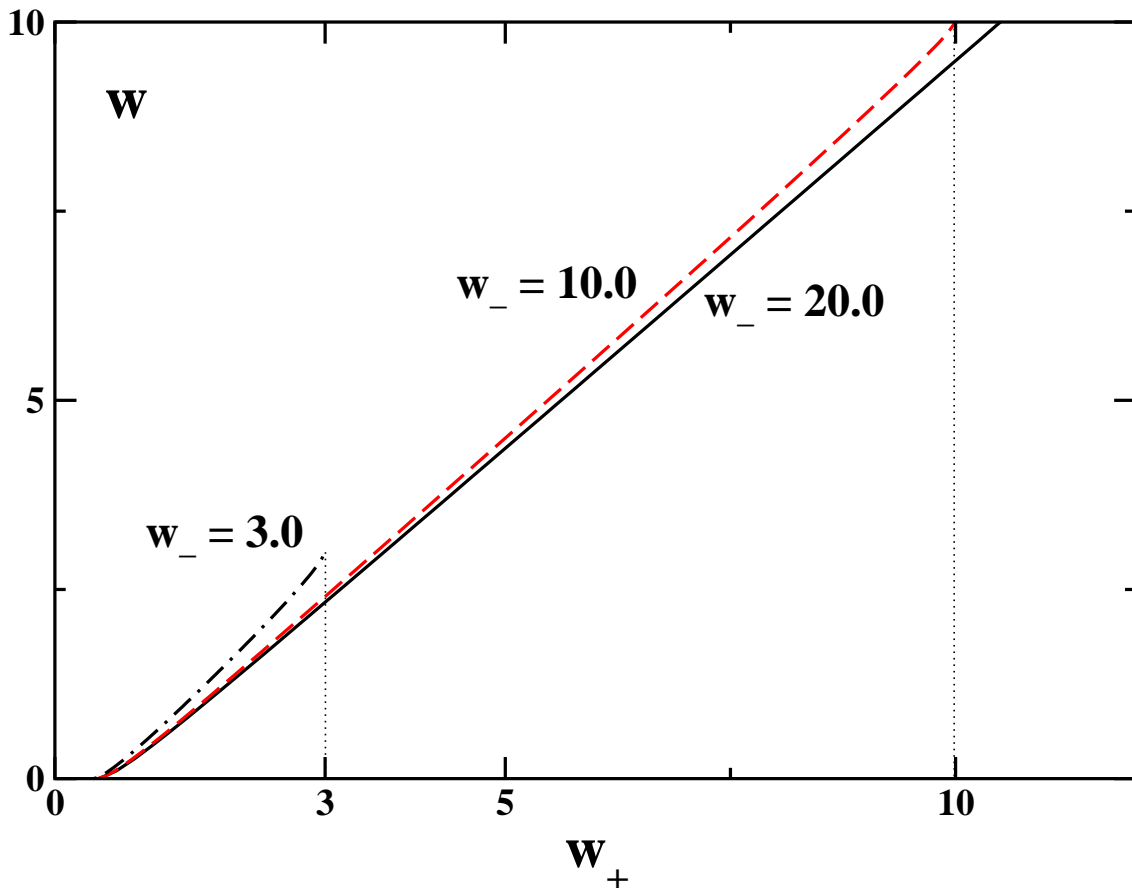


Figure 8: Dependencies of  $w$  on  $w_+$  for various values of the anchoring energy parameter  $w_-$ . It is shown that  $w = w_-$  at  $w_+ = w_-$  and  $w = 0$  at  $w_+ = w_c$  (see Eq. (32)).

It is now our task to study the dependence of the pitch wavenumber  $q$  on the free twist wavenumber  $q_0$ , which is proportional to the chiral parameter,  $q_0 = h/K$ , at different anchoring conditions. Equivalently, we concentrate on the dependence of  $\beta$  on  $\beta_0$  (see Eqs. (18) and (23)). This dependence can be thought of as a sort of dispersion relation.

### 3.1 Strong anchoring limit

First we consider the case of the strong anchoring limit,  $W_{\pm} = W \rightarrow \infty$ , that can be readily treated without recourse to numerical analysis. In this case the boundary conditions require the director at the substrates to be parallel to the corresponding easy axes,  $\hat{\mathbf{n}}(\pm l) \parallel \hat{\mathbf{e}}_{\pm}$ . This imposes the restriction on the values of  $q$ , so that  $q$  takes the values from a discrete set. This set represents locally stable director configurations labelled by the half-turn number  $m$  as follows

$$2ql = \Delta\phi + \pi m, \quad m \in \mathbb{Z}. \quad (28)$$

Substituting the values of  $\beta$  from the relation (28) into the first term on the right hand side of Eq. (24) will define the equilibrium value of  $m$  as the integer that minimizes the distance between  $\pi m$  and  $2q_0l - \Delta\phi$ . The resulting step-like dependence is depicted in Fig. 2a.

### 3.2 Equal anchoring energies

When the anchoring strengths at both substrates are equal,  $W_- = W_+ \equiv W$ , the right hand side of Eq. (23) is  $\beta \pm w \sin \beta$  ( $w = Wl/K$ ) and  $\psi_+ = \psi_- = \beta$ . So, as is illustrated in Fig. 3(a), we need to find the intersection points of the horizontal line  $\gamma = \beta_0$  and the curves  $\gamma = \gamma_{\pm}(\beta)$  in the  $\beta - \gamma$  plane. The stability conditions  $A_+ > 0$  and  $H_+ > 0$  ( $A_- > 0$  and  $H_- > 0$ ) require the values of  $\beta$  to be ranged between  $(m - 1/2)\pi$  and  $(m + 1/2)\pi$ , where  $m$  is even (odd) integer equal to the half-turn number. The function  $\gamma_+$  ( $\gamma_-$ ) monotonically increases on these intervals, so that the value of  $\beta_0$  runs from  $(m - 1/2)\pi - w$  to  $(m + 1/2)\pi + w$  on the interval with the half-turn number  $m$ :  $[(m - 1/2)\pi, (m + 1/2)\pi]$ . For each number of  $m$  we have the monotonically increasing branch of the  $\beta$  vs  $\beta_0$  dependence. The branches with  $m$  ranged from 10 to 14 for different values of the dimensionless anchoring energy parameter  $w$  are depicted in Fig. 2. It is illustrated that the  $\beta_0$ -dependence of  $\beta$  will be discontinuous provided the anchoring energy is not equal to zero. Fig. 2 shows that the jumps tend to disappear in the limit of weak anchoring, where the anchoring energy approaches zero,  $w \rightarrow 0$ .

Similar to the case of strong anchoring, at  $\beta_0 = \pi/2 + \pi m$  we have two different roots of Eq. (23) with  $k = m$  and  $k = m + 1$  that are equally distant from  $\beta_0$  and are of equal energy. According to Refs. [9, 10, 11, 12] it can be assumed that the jumps actually occur at the end points  $\beta_0 = \pi/2 + \pi k \pm w$ , where the configuration with  $m = k + 1/2 \mp 1/2$  becomes marginally stable ( $A_{\pm} = H_{\pm} = 0$ ) and loses its stability. In other words, the system needs to penetrate the barrier separating the states with different half-turn numbers. As it is seen from Fig. 2, in this case the upward and backward transitions with  $\Delta m = \pm 1$ :  $k \rightarrow k + 1$  and  $k + 1 \rightarrow k$  occur at different values of  $\beta_0$ :  $\beta_+^{(k)} = \pi/2 + \pi k + w$  and  $\beta_-^{(k)} = \pi/2 + \pi k - w$ , correspondingly. It means that there are hysteresis loops in the response of CLC to the change in the free twisting number.

When the anchoring energy is small and  $w < \pi/2$ , there are only two configurations at the critical point  $\beta_0 = \beta_+^{(k)}$ : the marginally stable configuration with  $m = k$  and the equilibrium one with  $m = k + 1$ . In this case Eq. (23) has at most two roots and the jumps will occur as transitions between the states which half-turn numbers differ by the unity,  $|\Delta m| = 1$ .

Fig. 4a illustrates that for  $w = \pi/2$  we have two marginally stable structures of equal energy with  $m = k$  and  $m = k + 2$ . Being metastable at  $\pi/2 < w < \pi$  this newly formed structure and the configuration with  $m = k + 1$  will be degenerate in energy at  $w = \pi$ . So, as is shown in Figs. 2b and 4b, both transitions  $k \rightarrow k + 1$  and  $k \rightarrow k + 2$  are equiprobable, so that we have the bistability effect at the critical point under  $w = \pi$ . For  $\pi < w < 2\pi$  the configuration with  $m = k + 2$  gives the equilibrium director structure at  $\beta_0 = \beta_+^{(k)}$ .

It is not difficult to see that further increase of the anchoring energy involves the configuration with  $m = k \pm l$  into the transition when the parameter  $w$  is passing through the value  $(l - 3/2)\pi$ . The jump to the equilibrium state will require the half-turn number changed from  $k$  to  $k + \Delta m$ ,

where  $|\Delta m| = l$  at  $(l - 1)\pi < w < l\pi$ . There are a number of transient metastable configurations involved in transitions with  $|\Delta m| < l$ .

### 3.3 Different anchoring energies

When the anchoring energies at the surfaces are different,  $W_- \neq W_+$ ,  $\sin \psi_+$  on the right hand side of Eq. (23) equals zero at  $\beta = \pi/2 + \pi k$  and, as is seen from Fig. 3b, we have additional intersection points of the curves  $\gamma_+(\beta)$  and  $\gamma_-(\beta)$ . The stationary points, where the derivative of  $\gamma_{\pm}$  with respect to  $\beta$  equals zero, represent the local maxima and minima of  $\gamma_{\pm}$  and are located at  $\beta = \pi/2 + \pi k \pm \Delta\beta$ . The value of  $\Delta\beta$  can be calculated by solving the following equation

$$w_+(1 + \epsilon) \sin(\Delta\beta - \epsilon \arctan[\epsilon \cot \Delta\beta]) = -\frac{1 + (\epsilon^2 - 1) \cos^2 \Delta\beta}{1 + (\epsilon - 1) \cos^2 \Delta\beta}, \quad (29)$$

where  $\Delta\beta \in [0, \pi/2]$ .

From the stability conditions  $H_+ > 0$  ( $H_- > 0$ ) the values of  $\beta$  for stable configurations fall between the stationary points  $(m - 1/2)\pi + \Delta\beta$  and  $(m + 1/2)\pi - \Delta\beta$ , where the half-turn number  $m$  is even (odd) integer. The function  $\gamma_+$  ( $\gamma_-$ ) monotonically increases and  $\beta_0$  varies from  $(m - 1/2)\pi - w$  to  $(m + 1/2)\pi + w$  on these intervals. The dimensionless parameter  $w$ , as opposed to the case of equal anchoring energies, is now given by

$$w = w_+ \cos(\Delta\beta - \epsilon \arctan[\epsilon \cot \Delta\beta]) - \Delta\beta. \quad (30)$$

Clearly, we can now follow the line of reasoning presented in the previous section to find out the results concerning hysteresis loops and bistability effects that are similar to the case of equal anchoring strengths. There are, however, two important differences related to Eqs. (29) and (30).

If  $\Delta\beta \neq 0$ , the intervals of  $\beta$  representing stable director configurations are separated by the gap of the length  $2\Delta\beta$ . The presence of this gap is illustrated in Figs. 5a and 5b. Fig. 6b shows the gap between stable branches of the dependence of the free energy on  $\beta$ . The values of  $\beta$  that are within the gap represent unstable configurations (“forbidden” states of CLC). The graph of the  $\Delta\beta$  vs  $w_+$  dependence is presented in Fig. 7 and indicates that the gap disappears in the limit of equal energies,  $w_+ = w_-$ . In addition, referring to Fig. 7, there is a critical value of  $w_+$  below which  $\Delta\beta$  equals zero.

It can be shown that Eq. (23) has the only root,  $\beta = \beta_0$  at  $\beta_0 = \pi/2 + \pi k$ , under the anchoring energies meet the following condition:

$$\sigma \equiv \frac{2w_- w_+}{|w_- - w_+|} \leq 1. \quad (31)$$

In this case the gap disappears and the dependence of  $\beta$  on  $\beta_0$  becomes continuous in the manner indicated in Figs. 5c and 5d. Given the value of  $w_-$  the relation (31) yields the threshold value

for the anchoring strength at the upper substrate. The critical anchoring energy parameter  $w_c$  is given by

$$w_c = \frac{w_-}{2w_- + 1}. \quad (32)$$

As illustrated in Fig. 8, the dependence of  $w$  on  $w_+$  is approximately linear for large values of  $w_-$  and  $w$  goes to zero at the critical point  $w_+ = w_c$ .

## 4 Conclusion

In this paper we have studied how the pitch wavenumber of CLC cell depends on the free twisting number for the cases in which the anchoring strengths at the substrates are either equal or different. It is found that in both cases this dependence is generally discontinuous and is characterized by the presence of hysteresis and bistability. But the difference in the anchoring energies introduces the following two effects:

- (a) the jump-like behaviour of the twist wavenumber is suppressed under the anchoring strength at one of the substrates is below its critical value;
- (b) the twist wavenumber intervals of locally stable configurations with adjacent numbers of the helix half-turns are separated by the gap where the structures are unstable.

The part of our analysis, presented in Sec. 3.2, relies on the assumption that the transition between configurations with different half-turn numbers occurs when the initial structure loses its stability, so that its pitch wavenumber no more corresponds to a local minimum of the free energy surface. The result is that the stronger the anchoring, the larger the change of the half-turn number (and of the twist wavenumber) needed to reach the equilibrium state. So, whichever mechanism of relaxation is assumed, the metastable states certainly play an important part in the problem. Dynamics of the transitions is well beyond the scope of this paper and it still remains a challenge to develop a tractable theory that accounts for director fluctuations, hydrodynamic modes and defect formation.

Analytical results of Sec. 2 can be used to study the effect of pretilt angles at the confining surfaces. This problem requires a more complicated analysis that will be published elsewhere.

## References

- [1] M. J. Stephen and J. P. Straley, *Rev. Mod. Phys.* **46**, 617 (1974).
- [2] P. G. de Gennes and J. Prost, *The Physics of Liquid Crystals* (Claderon Press, Oxford, 1993).
- [3] A. B. Harris, R. D. Kamien, and T. C. Lubensky, *Rev. Mod. Phys.* **71**, 1745 (1999).

- [4] A. B. Harris, R. D. Kamien, and T. C. Lubensky, Phys. Rev. Lett. **78**, 1476 (1997).
- [5] T. C. Lubensky, A. B. Harris, R. D. Kamien, and G. Yan, Ferroelectrics **212**, 1 (1997).
- [6] I. P. Pinkevich and V. Y. Reshetnyak, Zhurnal Tekhn. Fiz. **61**, 161 (1991) (in Russian).
- [7] I. P. Pinkevich, V. Y. Reshetnyak, and M. F. Lednei, Ukr. Fiz. Zhurnal **37**, 218 (1992) (in Russian).
- [8] I. P. Pinkevich, V. Y. Reshetnyak, Y. A. Reznikov, and L. G. Grechko, Mol. Cryst. Liq. Cryst. **222**, 269 (1992).
- [9] H. Zink and V. A. Belyakov, Mol. Cryst. Liq. Cryst. **265**, 445 (1995).
- [10] H. Zink and V. A. Belyakov, Mol. Cryst. Liq. Cryst. **329**, 457 (1999).
- [11] V. A. Belyakov and E. I. Kats, JETP **118**, 560 (2000) (in Russian).
- [12] S. P. Palto, JETP **121**, 308 (2002) (in Russian).
- [13] M. Abramowitz and I. A. Stegun, eds., *Handbook of Mathematical Functions* (Dover, New York, 1972).